Measurements and calculations of the energy fluence rate in a scattering and absorbing phantom at 633 nm

Christian J. M. Moes, Martin J. C. van Gemert, Willem M. Star, Johannes P. A. Marijnissen, and Scott A. Prahl

We have studied the influence of absorption, scattering, and refractive index of a phantom medium in conjunction with various beam diameters on the penetration depth of light at 633 nm. We used mixtures of Intralipid 10% (scattering medium) and Evans blue (absorbing medium). Measurements were performed in media with a scattering coefficient of 1 mm^{-1}, an anisotropy factor of 0.71, absorption coefficients of 1.3×10^{-3}, 0.01, and 0.05 mm^{-1}, and a refractive index of 1.33. The experimental results were compared with an analytical solution of the fluence rate based on diffusion theory. We found good agreement (deviations of <10%) between theory and experiment for incident beam diameters between 10 and 60 mm.

I. Introduction

One problem in clinical laser therapy is the prediction of the light distribution in tissue. Light propagation in tissue is complicated by the inhomogeneous and variable character of tissue. In addition, *in vitro* samples are expected to have different optical properties from *in vivo* samples. Since we wanted to investigate methods of measuring optical properties and computing fluence rates using these optical properties, we developed a phantom medium with reproducible optical properties. We investigated the influence of irradiation beam diameter, absorption, scattering, and refractive index of the medium on the energy fluence rate in a phantom medium at 633 nm. The experimental results are compared to calculations based on diffusion theory.

II. Materials and Methods

A. Theory

The light distribution in an absorbing and scattering medium is described by the radiative transfer equation, an integrodifferential equation describing the transport of light in turbid media.[1,2] General (analytic) solutions of this equation for the geometry of our experiment are not known. However, in certain conditions such as nearly diffuse radiation inside the medium, absorption much smaller than scattering, and the scattering phase function containing an isotropic part and a forwardly directed peak, it is possible to derive an analytic solution.[3,4] This solution contains only simple tissue parameters such as the absorption coefficient μ_a, scattering coefficient μ_s, asymmetry parameter g, index of refraction of the medium, and geometric parameters such as the diameter of the incident beam. We have used the diffusion approximation according to Groenhuis *et al.*[4] Based on this theory a computer program was developed which calculates fluence rates in a slab geometry for a finite width flat beam irradiance.[5]

B. Phantom Materials

Because biological tissues are often irregular and inhomogeneous, the measurements were performed in reproducible optical phantoms. Recent developments in the measurement of tissue parameters indicate that tissue scatters light strongly in the forward direction.[6,7] Therefore, we have chosen Intralipid 10% (Kabivitrum, Stockholm) which has highly forward scattering properties and low absorption (see Sec. V). From measurements of the particle size of Intralipid 10% with a Coulter-Counter (Coulter-Electronics model ZM) it appeared that the mean size of the particles and the standard deviation is 1.00 ± 0.14 μm.

As an absorber we used Evans blue dissolved in an isotonic phosphate buffer (515 mg/liter). By mixing different concentrations of both materials it is possible to obtain the desired optical parameters of the medium. We used the method described below to determine the optical properties of Intralipid.

W. M. Star and J. P. A. Marijnissen are with Dr. Daniel Den Hoed Cancer Center, Physics Department, 3008 AE Rotterdam, The Netherlands; and the other authors are with The Laser Center, Academic Medical Center, Amsterdam, The Netherlands.

Received 28 December 1988.
0003-6935/89/122292-05$02.00/0.

C. Measurement of μ_s and μ_a

To determine the scattering coefficient μ_s of Intralipid we used the experimental setup shown in Fig. 1. A cuvette of diameter d is filled with Intralipid and placed in a tank with clear water. The beam of a He–Ne laser (633 nm) is directed perpendicular to the cuvette, and the transmitted light is detected by a photodiode. The added absorber technique (Sec. II.D) shows that absorption of Intralipid is negligible. Consequently, the total attenuation coefficient μ_t ($=\mu_a + \mu_s$) is equal to the scattering coefficient. The total attenuation coefficient measurement must be performed with a very small detector acceptance angle to minimize scattered light detection. The acceptance angle β of the two pinholes I and II (see Fig. 1) was ~1 mrad in our experiment. We repeated the experiment for several concentrations of Intralipid; to avoid multiple scattering we measured at low concentrations (down to a 1% solution). To measure μ_s we made the assumption that for low concentrations single scattering applies so that we may use

$$E = E_0 \exp(-\mu_s \cdot c \cdot d), \tag{1}$$

where c is the concentration (100% is nondiluted Intralipid 10%), d is the diameter of the cuvette (we used two cuvettes with diameters of 5 and 10 mm), E is the irradiance (in W/m^2), and E_0 is the incident irradiance.

The scattering coefficient μ_s is now given by

$$\mu_s = -\frac{1}{d}\frac{\partial \ln(E/E_0)}{\partial c}, \tag{2}$$

which is the slope of a $\ln(E/E_0)$ vs c plot (see Fig. 2). The linearity of the data indicates that Eq. (1) is valid.

The final value found for μ_s was

$$\mu_s = (38.6 \pm 0.4) \times 10^{-3}\ \mathrm{mm}^{-1}/(\mathrm{mliter/liter}), \tag{3}$$

which is the scattering coefficient taken for a solution of 1-mliter Intralipid (10%)/liter of solvent. Thus for a concentration of 2% (which is 20 ml of Intralipid 10% in 1000 mliter of solvent) we find that $\mu_s = 0.772\ \mathrm{m}^{-1}$.

The absorption coefficient μ_a of Evans blue was found by a similar transmission measurement using the Beer-Lambert law yielding

$$\mu_a = (7.60 \pm 0.05) \times 10^{-3}\ \mathrm{mm}^{-1}/(\mathrm{mliter/liter}), \tag{4}$$

Comparing this value to the results from measurements using a spectrophotometer we found agreement within 2%.

D. Determination of g

The asymmetry parameter g was found using the so-called added absorber method. This method is based on the solution of the transport equation for a point source in an infinite medium in the diffusion approximation[2,8]:

$$\psi(r) = \frac{c}{r}\exp(-r \cdot \mu_{\mathrm{eff}}), \tag{5}$$

where $\psi(r)$ is the fluence rate in (W/m^2) at radius r, c is a constant, and

$$\mu_{\mathrm{eff}}^2 = 3\mu_a[\mu_a + (1-g)\mu_s]. \tag{6}$$

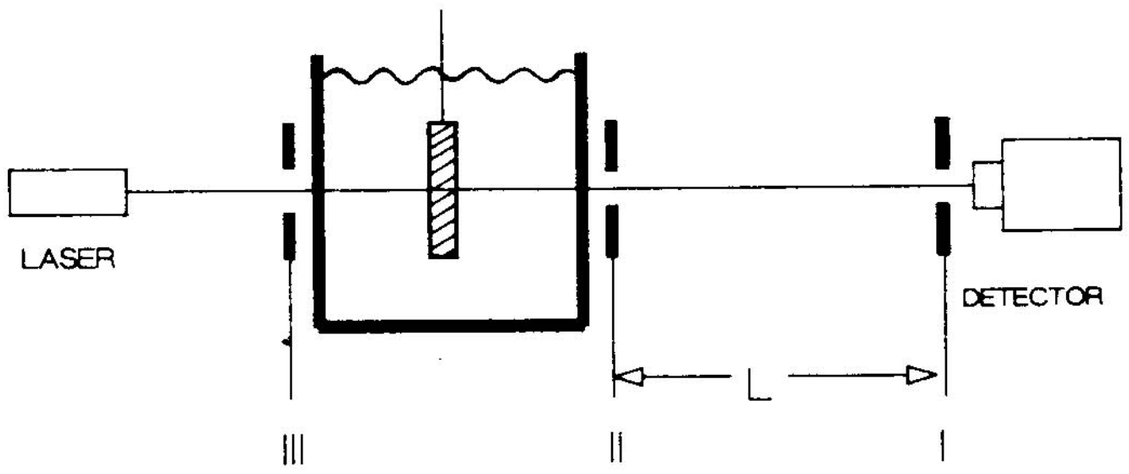

Fig. 1. Experimental setup for determination of μ_a and μ_s. I, II, and III are pinholes with diameters of 0.5, 1, and 1 mm, respectively; L is 2 m.

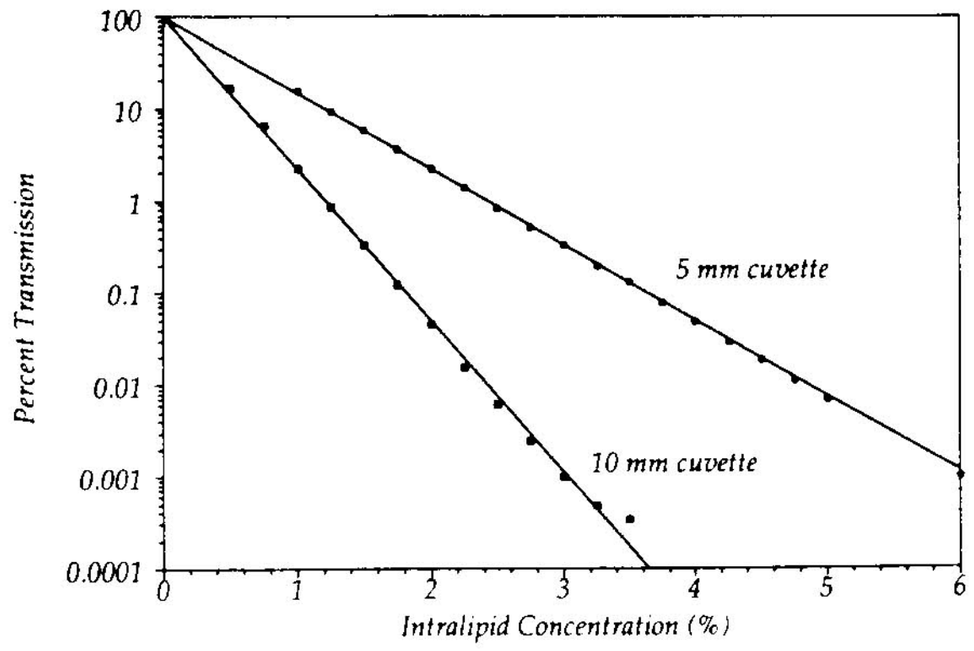

Fig. 2. Transmitted light as a function of the concentration of Intralipid.

From Eq. (5) we can determine the effective attenuation coefficient μ_{eff} by

$$\mu_{\mathrm{eff}} = -\frac{\partial}{\partial r}\ln(\psi \cdot r), \tag{7}$$

which is the slope of a $\ln(\psi \cdot r)$ vs r plot. Once μ_{eff} is found, we can calculate g by inverting Eq. (6):

$$g = 1 - \frac{\mu_a}{\mu_s}\left(\frac{\mu_{\mathrm{eff}}^2}{3\mu_a^2} - 1\right). \tag{8}$$

For our measurements we used the experimental setup shown in Fig. 3. A fiber with an isotropic radiating tip[6] is placed in a scattering and absorbing medium, and the energy fluence rate ψ is measured as a function of the radius r with an isotropic detecting fiber (a fiber identical to that used for the light source). The results are presented in Fig. 4. Measurements were performed for two scattering coefficients and several absorption coefficients (including no absorber added; see Fig. 4). From these measurements we find after an iterative process (where we use the calculated value of g in the fit of the data of pure Intralipid to determine the absorption of Intralipid μ_{a0}) both the asymmetry parameter g and absorption coefficient of pure Intralipid (10%):

$$g = 0.71 \pm 0.03; \tag{9}$$

$$\mu_{a0} = (5.7 \pm 1.5) \times 10^{-5}\ \mathrm{mm}^{-1}/(\mathrm{mliter/liter}). \tag{10}$$

Comparing these results of μ_s and g with those found by Star *et al.*[6] ($\mu_{s2\%} = 1.1\ \mathrm{mm}^{-1}$, $g = 0.83$), we find that,

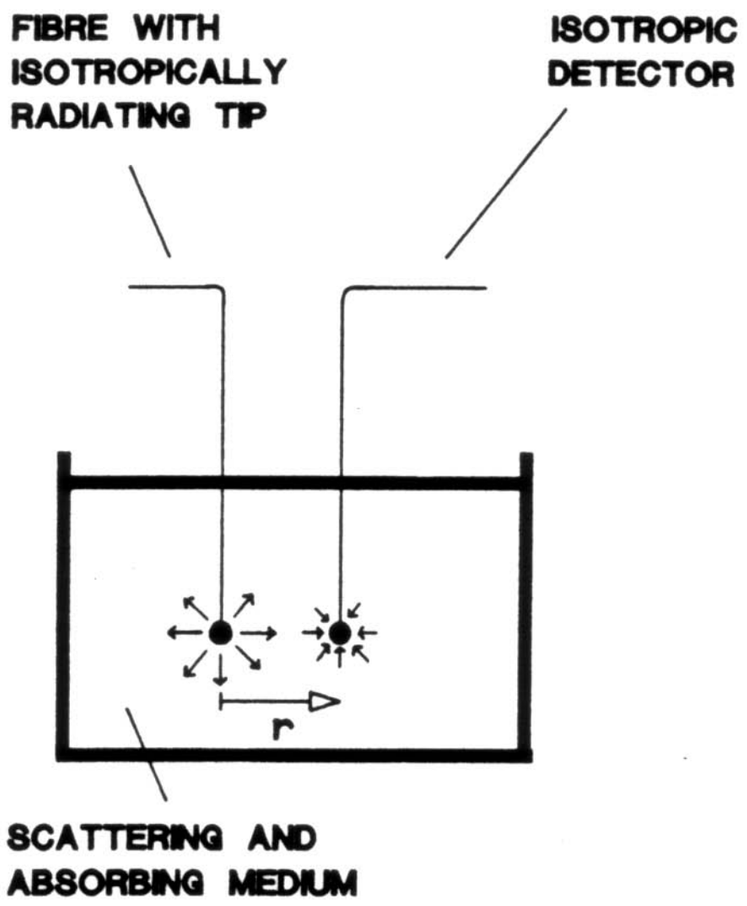

Fig. 3. Experimental setup for determination of the asymmetry parameter.

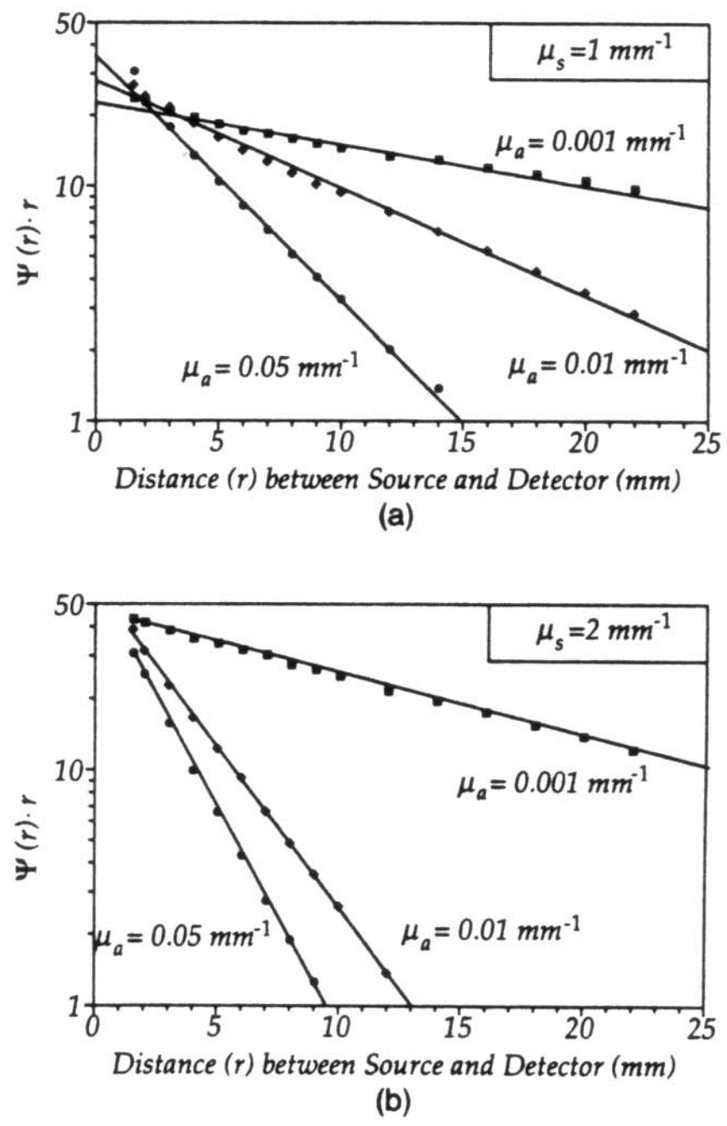

Fig. 4. (a) $\ln(\psi \cdot r)$ vs the r diagram of the detected fluence rate for $\mu_s = 1\ \text{mm}^{-1}$. (b) $\ln(\psi x \cdot r)$ vs the r diagram of the detected fluence rate for $\mu_s = 2\ \text{mm}^{-1}$.

although the values for μ_s and $(1 - g)$ differ substantially (40 and 70%, respectively), the value of $\mu_s(1 - g)$ differs by only 16%. An explanation for this difference could be a different kind of Intralipid 10%.

III. Measurement of Fluence Rate

Our measurements of the fluence rate in a scattering and absorbing medium as a function of depth and beam diameter were performed with the setup shown in Fig. 5. A laser beam (633 nm, 14 mW) is expanded by a microscope objective lens passed through a circular diaphragm and directed onto a Perspex tank filled with a scattering and absorbing medium. Measure-

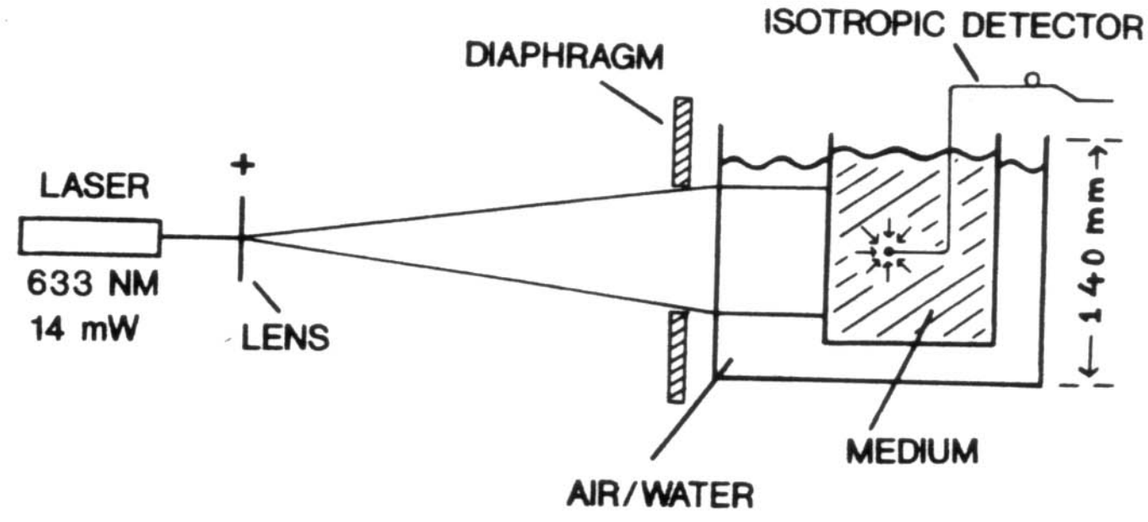

1. REFRACTIVE INDEX MATCHING
2. AIR-MEDIUM INTERFACE

Fig. 5. Experimental setup for the fluence rate measurements.

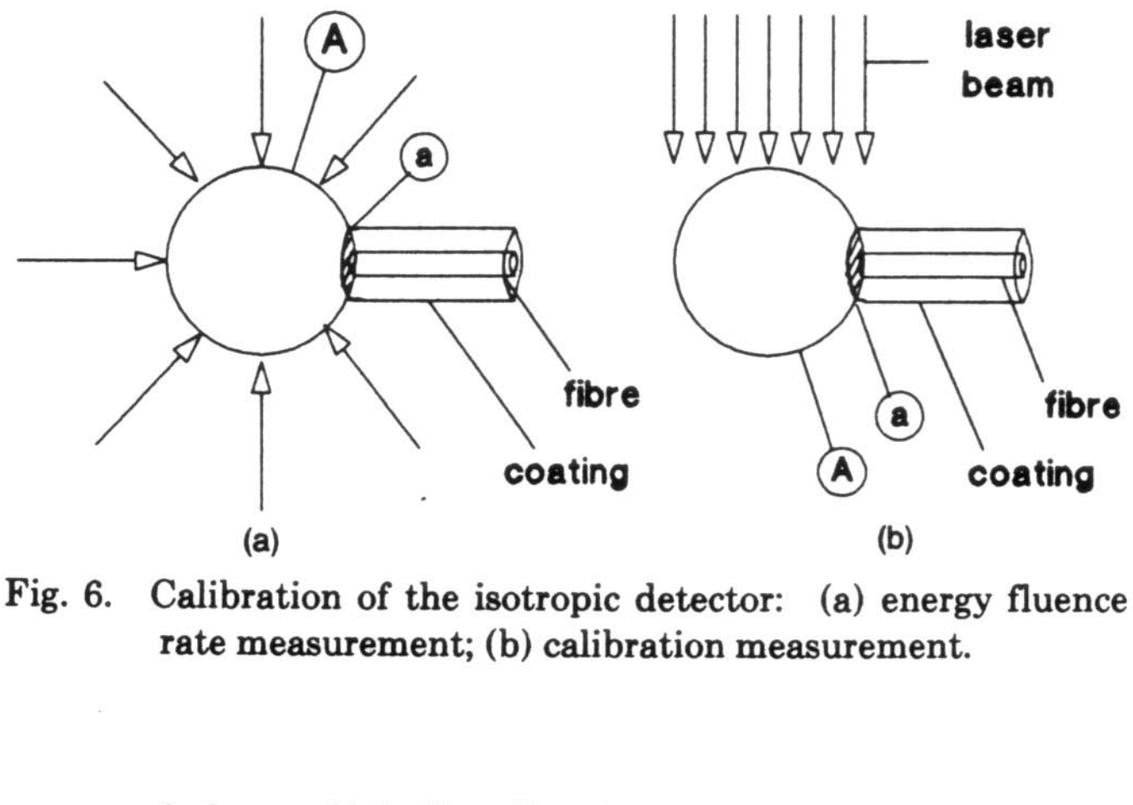

Fig. 6. Calibration of the isotropic detector: (a) energy fluence rate measurement; (b) calibration measurement.

ment of the radial distribution of the incident beam showed that, although the profile of the beam was Gaussian, the deviation from a uniform profile was small (<5%) and, therefore, comparable with computer calculations done with a flat irradiation profile. For index matched experiments this tank (12 × 14 × 14 cm) was filled with the Intralipid mixture and surrounded by another tank (16 × 18 × 20 cm) filled with clear water. To investigate the influence of the boundary conditions (the index mismatch between the Perspex tank and water was considered sufficiently small to be neglected) the outer tank was omitted. The light penetration was measured with an isotropic detector[6]; we measured the fluence rate along the center axis of the incident beam from the irradiation surface downward into the medium. The measurements were carried out in three phantom media with parameters $\mu_s = 1\ \text{mm}^{-1}$, $g = 0.71$, and $\mu_a = 1.3 \times 10^{-3}$, 0.01, and $0.05\ \text{mm}^{-1}$. We chose these values to obtain sufficient and measurable penetration of light, even though these parameters differ from real tissue parameters.

IV. Calibration of Isotropic Detector

In our experiments we measured the fluence rate inside the medium with respect to the fluence rate of the incident beam. A correction factor for the detector is, however, required. Consider the isotropic detector shown in Fig. 6 with surface area A. In an ideal

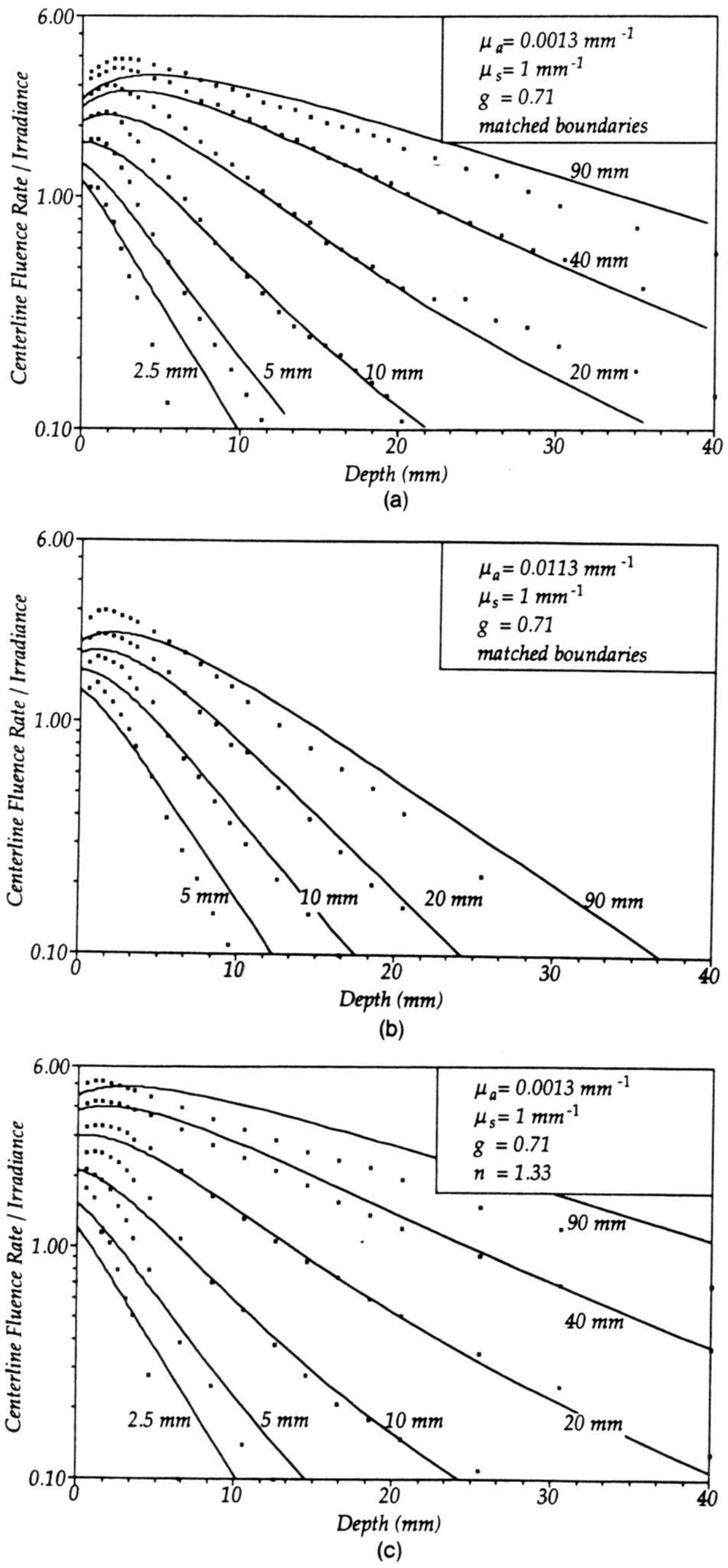

Fig. 7. (a) Fluence rate as a function of depth in the case of index matching. (b) Fluence rate as a function of the depth in the case of index matching. (c) Fluence rate as a function of the depth in the case of a refractive index mismatch.

situation this whole surface area A will be illuminated. However, when the energy fluence rate inside the medium is measured experimentally, the part of the detector which is connected to the fiber with cross section a is not illuminated [see Fig. 6(a)]. A correction factor is required because the connection of the detector to the fiber does not enter the calibration measurements, because in this case the fiber is perpendicular to the incident laser beam [see Fig. 6(b)]. Therefore, the relative energy fluence rate measurements inside the medium must be corrected by a factor $A/(A - a)$. In our case (with a detector diameter of 0.9 mm and fiber diameter of 0.65 mm) the correction factor is $A/(A - a)$ = 1.15. The results in Fig. 7 include this correction factor.

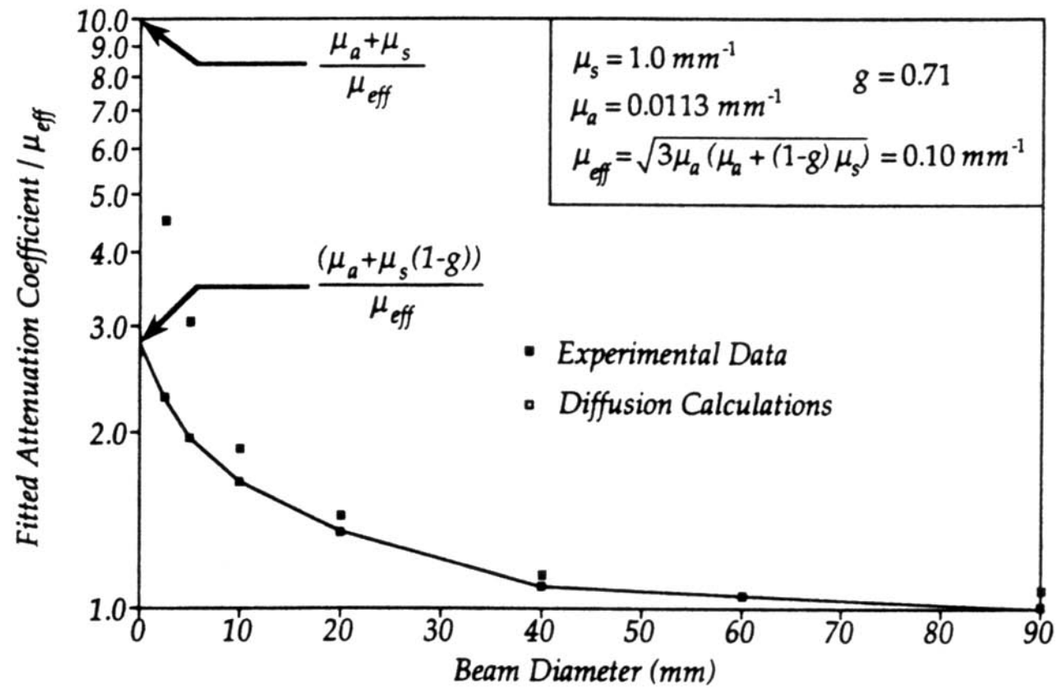

Fig. 8. Fitted attenuation coefficient for curves from Fig. 7(a) as a function of beam diameter in the case of index matching.

V. Results

In Figs. 7 some of the experimental results (single points) together with computer calculations based on diffusion theory (solid lines) are shown. Figures 7(a) and (b) show the results for refractive index matching for several beam diameters. The vertical axis gives the energy fluence rate along the axis of measurement inside the medium relative to the fluence rate of the incoming beam. The optical parameters of the phantoms are indicated in each figure. Figure 7(c) gives similar results but for the case of a refractive index mismatch at the boundary. In all three figures it appears that after a few optical depths, $\mu_t^{-1} = (\mu_a + \mu_s)^{-1}$, the fluence rate can be approximated by an exponential function.

Figure 8 shows the fitted attenuation coefficient (calculated by linear regression) of the curves in Fig. 7(b) as a function of the diameter of the incident beam. Figure 8 is typical of other figures showing this dependence. In this figure the (theoretically calculated) values of the effective attenuation coefficient μ_{eff} [see Eq. (6)], the transport coefficient $\mu_{\text{tr}} = \mu_a + (1 - g)\mu_s$ and the total attenuation coefficient $\mu_t = \mu_a + \mu_s$ are also shown.

VI. Discussion

From the results of Figs. 7 it appears that there is good agreement (differences of <10%) between the experimental values and the theoretical model for beam diameters between 10 mm and 60 mm (not shown in the figure). For small beam diameters (2.5 and 5 mm) the differences are larger (up to 50%); a reason for this difference will be given in the discussion of Fig. 8. The differences for large beam diameters are most likely caused by the size of the Perspex tank (12 × 14 × 14 cm) relative to the beam diameter (90 mm). Also there is a small difference between experimental values and theory for small depths ($z < 4$ mm); the cause for this difference could be the fact that we neglected the refractive index mismatch between Perspex tank and water in our calculations. Both Figs.

7(a) and (b) indicate that the energy fluence rate inside the medium is higher than the irradiance; this ratio can be as large as 5 depending on the amount of added absorber.

Comparing the results for index matching [Figs. 7(a) and (b)] with the results in the case of an air–medium boundary [Fig. 7(c)] we see a larger energy fluence rate in the latter case; this is caused by the higher internal reflection at the boundaries.

From the results of Figs. 7(a) and (b) it appears that after a few optical depths $\mu_t^{-1} = (\mu_a + \mu_s)^{-1}$ the fluence rate along the axis of measurement (see Fig. 5) can be approximated by an exponential function with an exponent depending on the diameter of the incident beam. In Fig. 8 this dependence is shown, and the results indicate that for a broad incident beam the fitted attenuation coefficient approaches μ_{eff}, in agreement with the diffusion theory. For very small incident beam diameters the fitted experimental attenuation coefficient tends to $\mu_t = \mu_a + \mu_s$, while the theoretical coefficient tends to $\mu_{\text{tr}} = \mu_a + (1 - g)\mu_s$. The reason for this difference is most likely that for small beam diameters the diffuse part of the fluence rate is much more forward peaked than for a wide beam (because there is little contribution to the diffuse fluence on the center line by light incident off the center line), and, therefore, the assumption in the diffusion approximation that the diffuse part can be approximated by a Taylor series and truncated after two terms[4] may not be valid anymore.

VII. Conclusions

We measured the optical parameters of Intralipid to be $\mu_s = (38.6 \pm 0.4) \times 10^{-3}$ mm^{-1}/(mliter/liter), $\mu_{a0} = (5.7 \pm 1.5) \times 10^{-5}$ mm^{-1}/(mliter/liter), and $g = 0.71$. We compared a 3-D diffusion approximation with results from several phantom media using these parameters for various beam diameters and for both refractive index matching and index mismatching. From the results it can be concluded that there is good agreement (deviations of <10%) between measurements and theory for beam diameters between 10 and 60 mm; larger differences for small and large beam diameters can be explained by the dimension of the detector and tank, respectively.

These results are not directly applicable to *in vivo* situations since we used phantoms with optical parameters different from tissue parameters. Nevertheless the results give a good indication of the light behavior inside the tissue.

References

1. S. Chandrasekhar, *Radiative Transfer* (Oxford U.P., London, 1960).
2. A. Ishimaru, *Wave Propagation in Random Media, Vol. 1* (Academic, New York, 1978).
3. L. O. Reynolds, C. Johnson, and A. Ishimaru, "Diffuse Reflectance from a Finite Blood Medium: Applications to the Modeling of Fiber Optic Catheters," Appl. Opt. **15,** 2059–2067 (1976).
4. R. A. J. Groenhuis, H. A. Ferwerda, and J. J. Ten Bosch, "Scattering and Absorption of Turbid Materials Determined from Reflection Measurements I and II," Appl. Opt. **22,** 2456–2467 (1983).
5. S. A. Prahl, "Light Transport in Tissue," Ph.D. Dissertation, U. Texas at Austin (1988).
6. W. M. Star, J. P. A. Marijnissen, H. Jansen, M. Keijzer, and M. J. C. Van Gemert, "Light Dosimetry for Photodynamic Therapy by Whole Bladder Irradiation," Photochem. Photobiol. **46,** 619–624 (1987).
7. S. L. Jacques, C. A. Alter, and S. A. Prahl, "Angular Dependence of He-Ne Laser Light Scattering by Human Dermis," Lasers Life Sci. **4,** 309–333 (1987).
8. W. M. Star, J. P. A. Marijnissen, and M. J. C. Van Gemert, "Light Dosimetry in Optical Phantoms and in Tissues. 1: Multiple Flux and Transport Theory," Phys. Med. Biol. **33,** 437–454 (1988).

I. Balslev, of Odense University, Denmark, photographed by W. J. Tomlinson, of Bellcore, at the International Conference on Optical Nonlinearity and Bistability of Semiconductors, East Berlin, in August 1988.